Effects of water depth on pumice formation in submarine domes at Sumisu, Izu-Bonin arc, western Pacific

Sharon R. Allen[1], Richard S. Fiske[2], and Yoshihiko Tamura[3]

[1]ARC Centre of Excellence in Ore Deposits, and School of Earth Sciences, University of Tasmania, Hobart, Tasmania 7001, Australia

[2]Smithsonian Institution, MRC-119, Washington, DC 20560, USA

[3]Japan Agency for Marine–Earth Science and Technology (JAMSTEC), 237-0061 2-15 Natsushima-cho, Yokosuka 237-0061, Japan

ABSTRACT

Domes of the Sumisu volcanic complex (western Pacific), having summits at ocean depths of 1100, 600, 245, and 95 m, are mantled with compositionally identical rhyolitic pumice that has similar vesicularity, but that varies systematically in distribution, size, and surface texture—suggesting that facies and morphology can serve as useful indicators of eruption depth. At depths >500 m, the pumice formed a thick carapace on dense rhyolite and disintegrated by quench fracture and mechanical failure into a jumble of giant (meters to tens of meters) polyhedral blocks with smooth curviplanar surfaces that display a single quenched margin. Vesiculation was arrested on eruption in seawater in all but the interior of the thickest carapace. At <500 m depths, the pumice occurs as an apron of blocky giant and smaller rough-textured clasts enclosed by quenched margins and pockmarked by coarse (cm) vesicles. No carapace pumice occurs, and the summit is composed of craggy dense dome rock. These shallower water pumice clasts resemble those spalled from historic submarine dome-forming eruptions that buoyed to the sea surface. We interpret spalling to result from vent-derived, weak volatile-driven explosions that take place at water depths <500 m. Our study shows that an increase in hydrostatic pressures over a range of 12 MPa reduces volatile-driven explosivity for subaqueous, rhyolitic, dome-forming eruptions, but does not affect vesicularity. We conclude that meter-size, highly vesicular pumice is diagnostic of subaqueous dome eruptions in water depths of at least 1300 m, and its morphology can be used to distinguish between explosive and effusive origins.

INTRODUCTION

At 1 atm, rhyolitic dome-forming eruptions typically begin explosively ejecting highly vesicular pumice lapilli and bubble-wall shards as a result of volatile overpressures in water-rich magmas (e.g., Eichelberger and Westrich, 1981; Fink et al., 1992; Eichelberger et al., 1986). Similar pumice has formed on the modern seafloor during phreatomagmatic eruptions in very shallow (less than a few tens of meters) water (e.g., the 1953–1957 Tuluman eruption—Reynolds et al., 1980; the 1934–1935 Showa Iwo-Jima eruption—Kano, 2003; the 2006 Home Reef eruption—Smithsonian Institution, 2006) and occurs in ancient volcanic successions (e.g., dome-tuff volcanoes; Cas et al., 1990). Eruptions from somewhat deeper vents were witnessed during the early phases of the 1934–1935 Showa Iwo-Jima and 1953–1957 Tuluman eruptions. Spalled giant pumice clasts rose to the sea surface hissing with steam (e.g., Reynolds et al., 1980; Kano, 2003). Spalled giant pumice clasts have also been produced during sublacustrine dome eruptions (e.g., Taupo eruption—Wilson and Walker, 1985; Sierra La Primavera—Mahood, 1980; Clough et al., 1981), and some examples occur in uplifted submarine arc successions (e.g., Allen and McPhie, 2000). Depth constraints and eruption mechanisms of spalling, however, are unknown.

Magmatic volatile-driven explosivity is controlled by the initial volatile content of the magma and the rate of decompression (McBirney, 1963; Wilson et al., 1980). Magmas erupted under water do not fully decompress because they are affected by the confining pressure of the overlying water column. Magmatic volatile exsolution is reduced with increasing water depth as a function of Henry's law. Hence, (1) explosivity tends to decrease as fewer volatiles are exsolved, and the volumetric expansion of steam is much lower at higher pressures, and (2) volatiles are retained in the melt, reducing its viscosity (McBirney, 1963; Mueller and White, 1992; White et al., 2003; Kano, 2003; Busby, 2005). Deeper eruptions are therefore thought to result in less vesicular pyroclasts and/or effusive, rather than explosive, eruptions (Busby, 2005), although deep-water explosions may be possible due to second-boiling induced by crystallization (e.g., Burnham, 1983; Downey and Lentz, 2006). In submarine settings, additional hydrovolcanic fragmentation processes operate, such as phreatomagmatic explosions in very shallow water and quench fragmentation in deep water (e.g., Pichler, 1965; Yamagishi, 1987).

Clarifying the effects of hydrostatic pressure on explosivity depends critically on comparing eruptions of similar magma composition and eruption intensity over a range of water depths, and this has not previously been attempted. We studied the products of four relatively small-volume, water-rich rhyolitic dome-forming eruptions in water depths spanning 1200 m. These domes are compositionally identical and mantled with highly vesicular pumice. We provide criteria to discriminate between deep-water (>500 m) and shallow-water (≤500 m) dome-derived pumice, and to distinguish between explosive and effusive origins. Our study shows that volatile-driven explosivity is reduced with increasing hydrostatic pressures over a range of 12 MPa, but this pressure range does not affect vesicularity.

Our results have the potential to further constrain eruption depths for submarine felsic dome eruptions in ancient and uplifted successions where the source is not preserved and/or in its eruptive setting. Previously, studies of facies associations have only allowed segregation into shallow- or deep-water sources based on indicators of storm-wave base, which lies within the range of 50–100 m water depth (Johnson and Baldwin, 1986).

GEOLOGICAL SETTING OF THE SUMISU VOLCANIC COMPLEX

The Sumisu volcanic complex occurs in the Izu-Bonin arc, immediately northeast of the actively extending Sumisu rift (Fig. 1). The complex is almost entirely submarine and includes an 8–9-km-diameter, ~90-m-deep caldera (Tani et al., 2008) and a cluster of rhyolitic domes that extend more than 25 km to the west. We here report on the study of four of these domes during research cruises undertaken by the Japan Agency for Marine-Earth Science and Technology (JAMSTEC) using remotely operating vehicles (ROVs), camera sleds (Deep-Tow), dredging, and multibeam seafloor swath-mapping.

The domes (labeled A, shallowest, to C, deepest) vary in size and summit ocean depths (Fig. 1). Dome A is a central summit dome, rising to 95 m below sea level (mbsl) on a broad 6 km^3 edifice (Dai-ichi Sumisu knoll). Dome A1 is a smaller, 245-m-high edifice on the southern part of Dai-ichi Sumisu knoll, rising from 490 to 245 mbsl. The lower parts of both domes A and A1 consist of steep (~40°) scree slopes containing either abundant giant (meter-sized) pumice clasts or small (<30 cm) pumice clasts and centimeter-sized dense rhyolite fragments, whereas the summits are craggy

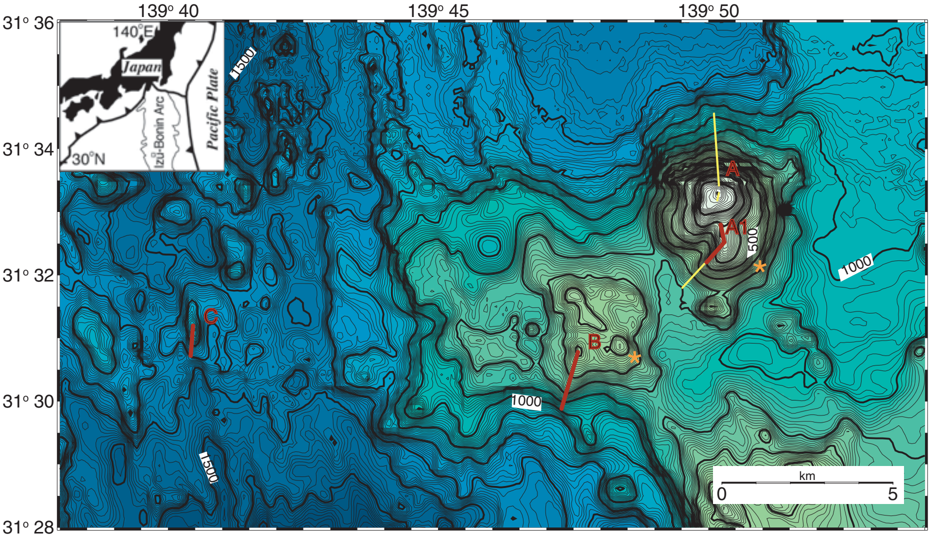

Figure 1. Bathymetry of western part of Sumisu volcanic complex and associated Sumisu back-arc rift, showing locations of four domes studied, deep-tow camera (yellow lines), remotely operated vehicle (ROV) traverses (red lines), and dredge sites (orange stars). Contour interval is 10 m.

C) however, differ markedly from those on the shallower-water (490–95 m) domes (A, A1). Domes B and C are both mantled by pumiceous carapace and a jumble of slabby giant pumice clasts, whereas domes A and A1 are surrounded by aprons of rough-textured, giant and smaller pumice clasts.

PUMICE CHARACTERISTICS

The intact pumice carapace of the deep-water domes (B, C) has relatively smooth upper quenched surfaces sporadically cut by meter-deep cracks (bread-crust texture) that reveal an internal hackly texture with curviplanar fracture surfaces (Fig. 2A). The carapace on the smallest, deepest dome (C) is ~2 m thick but is much thicker (>>3 m) on dome B. The thickest carapace is internally fractured with relatively regular decimeter-spaced columnar joints perpendicular to the quenched margin. Joint surfaces are curviplanar, and breakage along these joints forms slender prismatic columns (Fig. 2B). Vesicles of the carapace pumice are elongate

dense rhyolite. Pumice clasts cover the slopes of dome A to a depth of at least 1020 mbsl. Dome B is the southeastern dome of a 3.5 km^3 nested dome complex. It has a broad summit at 600 mbsl and 17°–24° margins that are mantled with a jumble of giant pumice clasts and rare intact pumiceous carapace to a depth of 1150 mbsl; no dense rhyolite was encountered. Dome C is a small (0.2 km^3), 200-m-high, free-standing edifice that rises from 1300 to 1100 mbsl. It consists of dense rhyolite encased by a thin pumiceous carapace. No obsidian was observed at any of the three domes.

Major- and trace-element compositions of pumice samples from domes A, A1, B, and C are virtually indistinguishable; all are high-Si rhyolites (76.0 ± 0.4 wt% SiO_2, 12.8 ± 0.2 wt% Al_2O_3, 1.21 ± 0.04 wt% K_2O recalculated anhydrous, 194 ± 7 ppm Zr). Phenocrysts make up 8 wt% and, in decreasing order of abundance, are plagioclase, quartz, orthopyroxene, and opaque minerals. H_2O and CO_2 measured by Fourier transform infrared spectroscopy in silicate glass melt inclusions within quartz crystals in pumice samples indicate that melt was trapped with similarly high water contents that ranged between 5.0 and 5.8 wt% and low CO_2 (<20 ppm) contents at all domes (Table 1). The GSA Data Repository[1] contains analytical methods and data.

The morphology and distribution of pumice at the two deep-water (1300–600 m) domes (B,

[1]GSA Data Repository item 2010110, methodology and data, is available online at www.geosociety.org/pubs/ft2010.htm, or on request from editing@geosociety.org or Documents Secretary, GSA, P.O. Box 9140, Boulder, CO 80301, USA.

TABLE 1. WATER CONTENTS IN MELT INCLUSIONS AND VESICULARITIES OF PUMICE AND DOME ROCK

Volcano	Depth (mbsl)*	H_2O content (wt%)†	σ	*n*	H_2O content exsolved (wt%)§	Vesicles (vol%) (melt) Theoretical#	Measured
A1	322	5.8	2	5	5.1	96	77.9
	434	5.4	1.2	7	4.5	93	81.4
B	876	5.1	0.8	7	3.9	85	77.5
	915	5.5	0.5	6	4.3	86	77.1
C	1161r	5.2	0.8	6	3.8	81	16.6
	1191	5.4	0.8	4	4	81	70.1
	1258r	5.0	0.3	4	3.5	78	4.83

*Collection depth, which is the minimum source depth due to downslope transport in scree; r is interior dome rock sample.
†Determined by Fourier transform infrared spectroscopy; *n* = number of melt inclusions.
§Based on the sample depth. Calculated by Henry's law, $ns = kp^2$ (Sparks, 1978), where *k* is the saturation constant for rhyolite (~4.11 × 10^{-6} Pa$^{-1/2}$), and *p* is pressure.
#Calculated from the wt% exsolved H_2O.

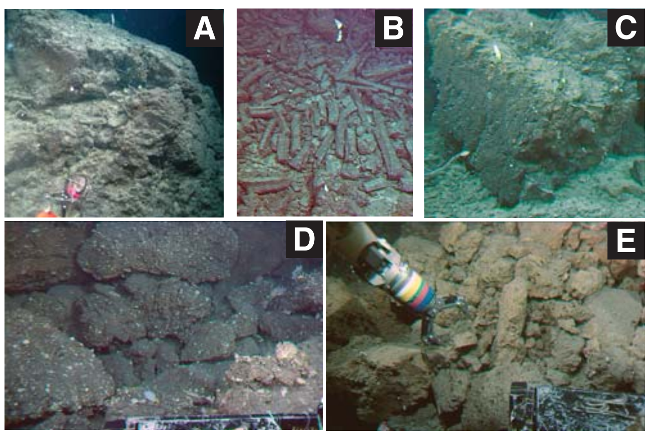

Figure 2. Pumice clasts and outcrops associated with submarine rhyolite domes. A: In situ pumiceous carapace on dome C at 1210 m; view is ~5 m wide. B: Scree slope of prismatic columns broken from carapace of dome B at 932 m; longest columns are ~1 m. C: Deep-water slabby giant pumice clast (diameter ~3 m) of dome B at 960 m. Surfaces show quenched wrinkled (left) and hackly broken (front, upper) surfaces. D: Rough-textured, giant (>2-m-diameter), shallower-water pumice clasts on dome A1 at 360 m. Yellow and white spots are sponge exoskeletons. E: Small (5–30 cm) shallower-water pumice clasts on dome A1 at 430 m.

parallel to the quenched margin. Some deep-water carapace pumice has a "woody" appearance (Kato, 1987) imparted by highly elongate vesicles. Abundant coarse (0.5–2 cm) vesicles are present in the interior of the thick columnar jointed carapace, whereas vesicles in the outer, 2–5-cm-thick quenched margin are smaller and less abundant. The carapace pumice is mostly white but includes millimeter-thick gray, less vesicular bands.

Deep-water giant pumice clasts are slabby, polyhedral blocks. One or up to a few of their margins are quenched and display roughly parallel, 2–5-cm-deep, centimeter-spaced wrinkle cracks and/or deeper decimeter-spaced curviplanar polygonal cracks. Internally, these cracks form normal joints (Fig. 2C). The remaining surfaces are both smooth and curviplanar or hackly. Edges and corners are angular to subangular. Associated small pumice clasts are equant and angular, and generally lack any quenched margins. Vesicle textures are more or less uniform throughout the pumice interior. The largest vesicles are generally <3 mm across.

The shallower-water giant and small pumice clasts are blocky and subangular to subrounded. Their surfaces are pitted with coarse vesicles (Figs. 2D and 2E). Most or all the surfaces are wrinkle-cracked by quench fractures. This coarsely vesicular surface texture occurs on both the giant and small clasts; however, quenched margins are less well developed as the clast size decreases. Interiors of giant pumice clasts have vesicle textures similar to the deep-water giant pumice (vesicles <3 mm, uniform distribution, and elongate). Interiors of smaller pumice clasts, however, have spherical vesicles and are coarsely vesicular.

Ranges of melt phase vesicularity in domes A and A1 (71–92 vol%), B (67–93 vol%), and C (70–83 vol%) are virtually identical, although dome C pumice does not attain the high vesicularities shown by domes A, A1, and B. Porosity and permeability measurements reveal that all pumice samples contain dominantly connected vesicles (92%–99%) and are highly permeable (gas permeabilities between 1×10^{-11} and 1×10^{-13} m^2; see the Data Repository). The dominant pumice texture consists of small (60–140 µm) vesicles with scattered medium (200–300 µm) and large (1–4 mm) vesicles and thin (4 µm) to thick (30 µm) vesicle walls. Vesicles have width-to-length ratios of 1:1.5–3. Pumice samples with the highest melt phase vesicularities (93 vol%) came from the prismatic columns of the thick carapace interior, as well as in some shallower-water small clasts (92 vol%). The prismatic columns are also dominated by medium (100–400 µm) and coarse (0.5–2 cm) vesicles and contain only <1 vol% isolated vesicles. Pumice samples with the lowest vesicularities include higher proportions of less vesicular gray bands.

CLAST FORMATION AND ERUPTION MECHANISMS

The deep-water slabby giant pumice clasts and small clasts appear to be fragments of pumiceous dome carapace. Their curviplanar surfaces indicate fracturing once the pumice had cooled below the glass transition temperature. Brittle fracture and mechanical failure of the quenched carapace probably accompanied dome growth, as documented for subaerial lavas (e.g., Fink, 1983). As dome disintegration was at depths well above the critical point of seawater (~3000 m; Bischoff and Rosenbauer, 1984), carapace breakup was presumably aided by formation of steam from seawater percolating into the hot dome interior through deep quench fractures (Fig. 3).

The evenly vesicular textures of the deep-water giant pumice clasts compared with the coarse vesicles within the carapace interior (prismatic columns) indicate that cooling of the broken carapace was rapid, and disintegration of the carapace arrested any further bubble growth and coalescence. Permeabilities and highly connected porosities suggest that ingestion of water would have been rapid once cooling commenced. Quenching causes the steam-filled vesicles in hot pumice to condense, promoting rapid water ingestion (Allen et al., 2008); therefore, these deep-water pumice clasts did not float to the sea surface. The summits of domes B (600 m) and C (1100 m) are the shallowest depths from which the deep-water slabby giant clasts could have originated. Similar in situ and broken carapace pumice has been observed at source depths up to 1600 m in the Okinawa Trough (Kato, 1987) and 2100 m in the eastern Manus Basin (Binns, 2003).

The morphology and vesicle textures of the shallower-water pumice clasts resemble giant and small spalled pumice clasts produced by historical eruptions in water depths of 100–500 m (e.g., 1924 Iriomote Island eruption, 1934–1935 Showa Iwo-Jima eruption; 1953–1957 Tuluman eruption; 1984 Kaitoku eruption; Kano, 2003). The enclosing quenched margins indicate that cooling continued after clast formation. The coarsely vesicular surfaces indicate that vesicle coalescence and rupture contributed to fragmentation. Hence, they are pyroclasts, but the 0.95–5 MPa confining pressures resulted in a bias toward production of very large pyroclasts (giant pumice) (Fig. 3). Fragmentation was much less violent than would be the case at atmospheric pressure.

The wide distribution of the shallower-water giant and small pumice clasts on domes A and A1 suggests that these clasts retained sufficient heat after fragmentation to remain steam-charged and rise buoyantly (e.g., Allen et al., 2008). Even though the water-saturated giant pumice clasts were internally fractured and weighed

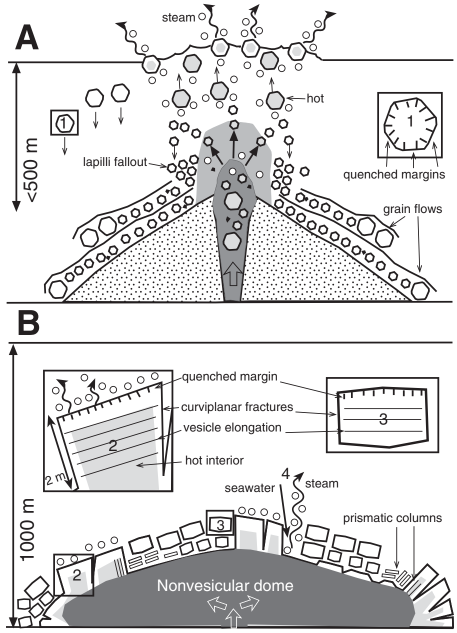

Figure 3. Contrasting eruption styles of water-rich, dome-forming rhyolite in shallow water (A) and deep water (B). A: Discrete, weak, pyroclastic eruptions generate giant and smaller pumice clasts that, once cooled, settle through water column. B: Vesiculated magma froths on the seafloor, generating a pumiceous carapace that breaks apart during dome growth. 1—Cooled giant pumice; 2—In situ pumiceous carapace; 3—Giant pumice slab; 4—Possible hydrovolcanic explosions.

tens to hundreds of kilograms, many remained largely intact upon settling, as their water-saturated densities would have been on average only 1.36× that of seawater. The volume of pumice produced by the shallower-water eruptions was also greater, forming thick aprons of pumice with steep slopes to depths of 1000 m. Transport by grain flows caused size segregation of giant pumice clasts into lobe fronts. We predict that these thick pumice aprons are internally bedded and fines poor, and they resemble bedded, well-sorted pumice observed in the caldera wall at 500–900 mbsl at Myojin Knoll caldera (Fiske et al., 2001), and >300–150 mbsl at Kolumbo volcano (Carey et al., 2008), and in the uplifted 120-m-thick pumice succession at Yali (Allen and McPhie, 2000).

Domes B and C erupted in 1300–600-m-deep water. The high (5.0–5.8 wt%) water contents of the Sumisu rhyolite magma allowed vesiculation even in the deepest dome, despite the greater confining pressure (Table 1). Their pumice is highly vesicular (67–93 vol%), similar to the shallower-water pumice from domes A and A1. However, there was no progression to an explosive eruption at domes C and B because the high confining pressure (13–6 MPa) reduced bubble overpressures to less than the tensile strength of the magma and/or reduced the magma rise rate. Instead, the volatile-rich magma erupted effusively as foaming lava. In comparison, eruption of domes A and A1 in shallower (490–95 m) water at lower (5–0.95 MPa) confining pressures allowed both vesiculation of the magma and vent-derived magmatic volatile-driven explosions. Most of the shallower-water pumice was erupted as pyroclasts at this dome, so the domes lack a pumiceous carapace. Hence, highly vesicular pumice was erupted from vents spanning 1200 m of water depth. In subaerial settings, magmas with such high water contents would normally explode.

Pumiceous carapaces on subaerial domes result from eruption of a highly inflated magmatic foam (Eichelberger et al., 1986; Fink, 1983) or from posteruptive inflation in response to volatile migration (Fink and Manley, 1987; Fink et al., 1992). The magma erupted at the Sumisu domes must have vesiculated prior to eruption and erupted as foam because direct contact with cold seawater quenched the exterior and arrested vesiculation. Confining pressures >0.95 MPa were also far greater than the ~10 m lithostatic pressure thought to control the depth of vesiculation of the finely vesicular carapace (Fink and Manley, 1987). Instead, our results indicate that vesiculation of water-rich rhyolite is affected by the confining pressure in which it erupts. Reduced volatile exsolution in deeper water reduces the volume of pumice produced and thus may reduce ascent rates, allowing degassing and eruption of dense dome interiors.

CONCLUSIONS

The Sumisu rhyolite magma was sufficiently water rich to inflate and form highly vesicular pumice at water depths down to at least 1300 m. Magmatic volatile-driven eruptions, however, were suppressed by hydrostatic pressure at depths exceeding 500 m. Instead of exploding in deep water, the vesiculating magma foamed as it erupted and then quenched and partly disintegrated to form distinctive, 5–10 m slabs of giant pumice. Similar water-rich rhyolite that erupted in water depths <500 m exploded weakly, forming spalled pyroclasts dominated by giant pumice. We infer that confining pressure controlled the eruption style (explosive versus effusive) and the mechanisms by which the domes disintegrated. Our study shows that an increase in hydrostatic pressures over a range of 12 MPa reduces volatile-driven explosivity for rhyolitic dome-forming eruptions, but does not affect vesicularity.

ACKNOWLEDGMENTS

We thank the scientific and technical parties and crew of R/V *Kaiyo* and R/V *Natsushima*. J. McPhie, R. Berry, T. Simkin, and two anonymous reviewers provided constructive reviews of a previous version. Allen is an Australian Research Council Research Fellow.

REFERENCES CITED

Allen, S.R., and McPhie, J., 2000, Water-settling and resedimentation of submarine rhyolitic pumice at Yali, eastern Aegean, Greece: Journal of Volcanology and Geothermal Research, v. 95, p. 285–307, doi: 10.1016/S0377-0273(99)00127-4.

Allen, S.R., Fiske, R.S., and Cashman, K.V., 2008, Experimental quenching of steam-filled silicic pumice: Implications for submarine pyroclastic volcanism: Earth and Planetary Science Letters, v. 274, p. 40–49, doi: 10.1016/j.epsl.2008.06.050.

Bischoff, J.L., and Rosenbauer, R.J., 1984, The critical point and two-phase boundary of seawater, 200–500 °C: Earth and Planetary Science Letters, v. 68, p. 172–180, doi: 10.1016/0012-821X(84)90149-3.

Binns, R.A., 2003, Deep marine pumice from the Woodlark and Manus Basins, Papua New Guinea, *in* White, J., et al., eds., Explosive Subaqueous Volcanism: American Geophysical Union Geophysical Monograph 140, p. 329–343.

Burnham, C.W., 1983, Deep submarine pyroclastic eruptions, *in* Omoto, H., and Skinner, B.J., eds., The Kuroko and Related Volcanogenic Massive Sulfide Deposits: Economic Geology Monograph 5, p. 142–148.

Busby, C., 2005, Possible distinguishing characteristics of very deepwater explosive and effusive silicic volcanism: Geology, v. 33, p. 845–848, doi: 10.1130/G21216.1.

Carey, S., Sigurdsson, H., and 12 others, 2008, Submarine pyroclastic deposits from Kolumbo Volcano, Santorini Volcanic Field, *in* Understanding Volcanoes: International Association of Volcanology and Chemistry of the Earth's Interior, 2008 General Assembly, Reykjavik, Iceland, Scientific Programme (abstract), p. 68.

Cas, R.A.F., Allen, R.F., Bull, S.W., Clifford, B.A., and Wright, J.V., 1990, Subaqueous, rhyolitic dome-top tuff cones: A model based on the Devonian Bunga Beds, southeastern Australia and a modern analogue: Bulletin of Volcanology, v. 52, p. 159–174, doi: 10.1007/BF00334802.

Clough, B.J., Wright, J.V., and Walker, G.P.L., 1981, An unusual bed of giant pumice in Mexico: Nature, v. 289, p. 49–50, doi: 10.1038/289049a0.

Downey, W.S., and Lentz, D.R., 2006, Modelling of deep submarine pyroclastic volcanism: A review and new results: Igneous Rock Associations Volume 6: Geoscience Canada, v. 33, no. 1, p. 5–24.

Eichelberger, J.C., and Westrich, H.R., 1981, Magmatic volatiles in explosive rhyolitic eruptions: Geophysical Research Letters, v. 8, p. 757–760, doi: 10.1029/GL008i007p00757.

Eichelberger, J.C., Carrigan, C.R., Westrich, H.R., and Price, R.H., 1986, Non-explosive silicic volcanism: Nature, v. 323, p. 598–602, doi: 10.1038/323598a0.

Fink, J.H., 1983, Structure and emplacement of a rhyolitic obsidian flow; Little Glass Mountain, Medicine Lake Highland, northern California: Geological Society of America Bulletin, v. 94, p. 362–380, doi: 10.1130/0016-7606(1983)94<362:SAEOAR>2.0.CO;2.

Fink, J.H., and Manley, C.R., 1987, Origin of pumiceous and glassy textures in rhyolite flows and domes, *in* Fink, J.H., ed., The emplacement of Silicic Domes and Lava Flows: Geological Society of America Special Paper 212, p. 77–88.

Fink, J.H., Anderson, S.W., and Manley, C.R., 1992, Textural constraints on effusive silicic volcanism: Beyond the permeable foam model: Journal of Geophysical Research, v. 97, p. 9073–9083, doi: 10.1029/92JB00416.

Fiske, R.S., Naka, J., Iizasa, K., Yuasa, M., and Klaus, A., 2001, Submarine silicic caldera at the front of the Izu-Bonin arc, Japan: Voluminous seafloor eruptions of rhyolite pumice: Geological Society of America Bulletin, v. 113, p. 813–824, doi: 10.1130/0016-7606(2001)113<0813:SSCATF>2.0.CO;2.

Johnson, H.D., and Baldwin, C.T., 1986, Shallow siliciclastic seas, *in* Reading, H.G., ed., Sedimentary Environments and Facies: Oxford, Blackwell, p. 229–282.

Kano, K., 2003, Subaqueous pumice eruptions and their products: A review, *in* White, J., et al., eds., Explosive Subaqueous Volcanism: American Geophysical Union Geophysical Monograph 140, p. 213–230.

Kato, Y., 1987, Woody pumice generated with submarine eruption: Journal of the Geological Society of Japan, v. 77, p. 193–206.

Mahood, G.A., 1980, The geological evolution of a late Pleistocene rhyolitic center: The Sierra La Primavera, Jalisco, Mexico: Journal of Volcanology and Geothermal Research, v. 8, p. 199–230, doi: 10.1016/0377-0273(80)90105-5.

McBirney, A.R., 1963, Factors governing the nature of submarine volcanism: Bulletin of Volcanology, v. 26, p. 455–469, doi: 10.1007/BF02597304.

Mueller, W., and White, J.D.L., 1992, Felsic fire fountaining beneath Archean seas: Pyroclastic deposits of the 2730 Ma Hunter Mine Group, Quebec, Canada: Journal of Volcanology and Geothermal Research, v. 54, p. 117–134, doi: 10.1016/0377-0273(92)90118-W.

Pichler, H., 1965, Acid hyaloclastites: Bulletin of Volcanology, v. 28, p. 293–310, doi: 10.1007/BF02596934.

Reynolds, M.A., Best, J.G., and Johnson, R.W., 1980, 1953–57 Eruption of Tuluman Volcano: Rhyolitic Volcanic Activity in the Northern Bismarck Sea: Geological Survey of Papua New Guinea Memoir 7, 44 p.

Smithsonian Institution, 2006, Home Reef: Bulletin of the Global Volcanism Network, v. 31, http://www.volcano.si.edu/ (December 2009).

Sparks, R.S.J., 1978, The dynamics of bubble formation and growth in magmas: A review and analysis: Journal of Volcanology and Geothermal Research, v. 3, p. 1–37, doi: 10.1016/0377-0273(78)90002-1.

Tani, K., Fiske, R.S., Tamura, Y., Kido, Y., Naka, J., Shukuno, H., and Takeuchi, R., 2008, Sumisu volcano, Izu-Bonin arc, Japan: Site of a silicic caldera-forming eruption from a small open-ocean island: Bulletin of Volcanology, v. 70, p. 547–562, doi: 10.1007/s00445-007-0153-2.

White, J.D.L., Smellie, J.L., and Clague, D.A., 2003, Introduction, *in* White, J., et al., eds., Explosive Subaqueous Volcanism: American Geophysical Union Geophysical Monograph 140, p. 1–24.

Wilson, C.J.N., and Walker, G.P.L., 1985, The Taupo eruption, New Zealand. I: General aspects: Philosophical Transactions of the Royal Society of London, ser. A, v. 314, p. 199–228, doi: 10.1098/rsta.1985.0019.

Wilson, L., Sparks, R.S.J., and Walker, G.P.L., 1980, Explosive volcanic eruptions: IV. The control of magma properties and conduit geometry on eruption column behaviour: Geophysical Journal of the Royal Astronomical Society, v. 63, p. 117–148.

Yamagishi, H., 1987, Studies on the Neogene subaqueous lavas and hyaloclastites in southwest Hokkaido: Reports of the Geological Survey of Hokkaido, v. 59, p. 55–117.

Manuscript received 2 July 2009
Revised manuscript received 12 November 2009
Manuscript accepted 13 November 2009

Printed in USA